Applied Catalysis B: Environmental 238 (2018) 346–357

Contents lists available at ScienceDirect

Applied Catalysis B: Environmental

journal homepage: www.elsevier.com/locate/apcatb

First pilot scale study of basic *vs* acidic catalysts in biomass pyrolysis: Deoxygenation mechanisms and catalyst deactivation

K.G. Kalogiannis[a,*], S.D. Stefanidis[a], S.A. Karakoulia[a], K.S. Triantafyllidis[b], H. Yiannoulakis[c], C. Michailof[a], A.A. Lappas[a]

[a] Chemical Process and Energy Resources Institute, CERTH, P.O. Box 60361, Thermi, 570 01 Thessaloniki, Greece
[b] Department of Chemistry, Aristotle University of Thessaloniki, 541 24 Thessaloniki, Greece
[c] Grecian Magnesite S.A., Research Center, Vasilika, 570 06, Thessaloniki, Greece

ARTICLE INFO

Keywords:
Biomass catalytic pyrolysis
Ketonization
Aldol condensation
Base catalysts
Magnesium oxide

ABSTRACT

In order for catalytic biomass pyrolysis to be economically sustainable, low cost and highly efficient catalysts are needed. In a previous work, Magnesium oxide (MgO) basic catalysts produced from natural magnesite ($MgCO_3$) were found to be highly efficient alternatives to zeolitic catalysts which apart from their relatively high cost, they are easily deactivated due to biomass alkali deposition. In order to validate these findings in pilot scale, these natural MgO catalysts were investigated in a circulating fluidized bed pilot scale unit and were compared to a commercially available ZSM-5 catalyst. This is to the best of our knowledge the first attempt to evaluate a basic catalyst in biomass fast pyrolysis in a pilot unit employing commercially relevant process technology. The basic sites of the MgO catalysts enhanced ketonization and aldol condensation reactions, as it was verified by 2DGC-TOFMS analyses of the produced bio-oils. Deoxygenation was achieved mainly via formation of CO_2, while H_2O yield was substantially reduced in comparison to the ZSM-5 catalyst. As a result, bio-oils richer in hydrogen were obtained by the use of MgOs. However, the MgO catalysts led to a significant increase of the catalytically produced coke compared to ZSM-5. The effect of MgO properties, such as surface area and basicity on product yields and bio-oil composition was elaborated. In contrast to the acidic ZSM-5, no alkali metals were found to deposit on MgO, indicating different deactivation mechanisms between acidic and basic catalysts in biomass fast pyrolysis.

1. Introduction

The continuous increase in world energy demand, especially in the form of liquid fuels needed for transportation has increased the interest in exploiting biomass as an alternative energy source [1,2]. Lignocellulosic biomass is a low-cost, abundant and renewable energy source, which can be converted via thermochemical processes such as fast pyrolysis into liquid, gas and solid products.

Biomass fast pyrolysis produces liquid oil, known as bio-oil, which is considered a very promising biofuel/bioenergy carrier and a renewable source of high added value chemicals [3]. Bio-oil is a complex mixture of hundreds of different compounds originating from the thermal decomposition of cellulose, hemicellulose and lignin that constitute lignocellulosic biomass [4]. Among those chemical compounds are acids, ketones, aldehydes and other oxygenates which confer undesirable properties to the bio-oil such as low calorific value, corrosivity, instability under storage and immiscibility with hydrocarbon fuels [5].

Several technologies, targeting the upgrading to bio-oil through deoxygenation, have been proposed ranging from catalytic in situ pyrolysis [6–8] to hydrotreating the produced bio-oils in order to produce diesel and gasoline [9]. In situ catalytic pyrolysis is one of the most interesting options for upgrading bio-oil due to its simplicity, low capital cost when existing refinery infrastructure is used to integrate the produced bio-oil and high efficiency [10]. Many different heterogeneous catalysts have been tested in bio-oil vapor upgrading ranging from zeolites [11], metal oxides [12], mesoporous acidic materials [13,14] and metal doped zeolites [6,15].

Work in the literature has focused thus far on acidic catalysts that favor deoxygenation mostly via decarbonylation and dehydration reactions while enhancing production of aromatic compounds such as Benzene, Toluene and Xylene (BTX). Among the acid catalysts tested so far, ZSM-5 zeolite is the most frequently studied catalyst and considered the most efficient. Due to its unique three-dimensional microporous structure and relatively strong Brønsted acidity, it maximizes the yield

* Corresponding author.
E-mail address: kkalogia@cperi.certh.gr (K.G. Kalogiannis).

https://doi.org/10.1016/j.apcatb.2018.07.016
Received 5 April 2018; Received in revised form 2 July 2018; Accepted 5 July 2018
Available online 17 July 2018
0926-3373/

of aromatic hydrocarbons and minimizes the formation of coke [16]. However, alkali metals such as K, Na, Mg and Ca that are commonly found in biomass as residual ash are deposited on the acid sites of the catalyst, rendering it inactive and less selective. In addition, hydrothermal deactivation, enhanced by increased coke and char production results in further loss of activity of the catalyst [17]. The high catalyst deactivation rate, and hence its makeup rate [10], combined with the high zeolite price, ~ 5000 euros/ton for ZSM-5, can therefore render the technology economically unsustainable.

Considering the above, nature-derived minerals present significant advantages, such as significantly lower cost and minimal environmental footprint. Furthermore, they possess basic rather than acidic active sites and therefore they may be more resistant (or less affected by) to deactivation by alkali metal deposition. The basic active sites can catalyze different types of reactions, such as carbon coupling (C−C) reactions, which convert low molecular weight compounds, such as organic acids, aldehydes and ketones to diesel and gasoline range products. Basic catalysts promote the deoxygenation of pyrolysis vapors via the production of CO_2, which is a more efficient pathway with respect to carbon conservation than the production of CO that acidic catalysts promote. They also reduce H_2O production, thus conserving hydrogen in the bio-oil, increasing its energy content and quality. At this point, it should be noted that basic catalysis has not been thoroughly investigated as an alternative to acidic catalysis and to the best of our knowledge, there are no reported studies involving use of basic catalysis in biomass pyrolysis in pilot scale.

Nokkosmaki et al. [18] applied ZnO in catalytic pyrolysis. They found that ZnO was a mild catalyst, increasing gas yield only by 2 wt.%. However, the stability of the catalytic oil was significantly increased. Other metal oxides such as CaO and Fe_2O_3 [19], TiO_2 and ZrO_2/TiO_2 [20] were found to be very promising for biomass pyrolysis, achieving bio-oil oxygen reduction through the condensation of acids and aldehydes towards linear and cyclo- pentanones, reduction of the heavy fraction of the bio-oil and increase of the hydrocarbons yield. Recently, strongly basic zeolites have been synthesized from reaction of zeolites with ammonia at elevated temperatures, providing unique activity and selectivity for base-catalyzed reactions [21]. Such basic zeolites, e.g. amine-substituted ZSM-5, are also suggested as promising candidate catalysts for biomass conversion to hydrocarbons via catalytic pyrolysis [22]. However, the basic zeolites produced so far are unstable under biomass pyrolysis conditions and easily revert to their previous state during regeneration, where catalytic coke is burnt under high temperature oxidation conditions. Coupled with the high cost of synthetic zeolites it is obvious that this is an expensive alternative for the process of biomass pyrolysis.

Our group has also worked with basic materials such as TiO_2, ZrO_2/TiO_2 and MgO [12]. These types of materials enhance different deoxygenation pathways compared to acidic zeolites. Specifically, high CO_2 yields were observed, along with high yields of ketones in the liquid products, especially cyclopentanones and cyclopentenones. CO_2 and ketones production were attributed mainly to aldol condensation and ketonization reactions [23]. These carbon coupling (C−C) reactions are considered to be very beneficial since they condensate smaller aldehyde and acid molecules towards larger molecules with molecular weights closer to those of liquid transportation fuels. For the above reasons and in an effort to minimize catalyst cost, MgO materials derived from the simple calcination of Greek natural magnesites, without any further treatment, were studied on bench scale [24]. The materials' properties, structure, composition, porosity, morphology and surface area were thoroughly examined. It was found that the physicochemical properties of the MgO catalysts could be tailored to some extent depending on the production conditions (duration and temperature of calcination) and the characteristics of the parent Magnesite mineral. Overall, a variety of different materials were investigated as catalysts in biomass pyrolysis, some of which were found to be very promising when compared to a ZSM-5 catalyst.

In this work, selected natural MgO catalysts based on the results of the previous bench scale study were evaluated in a circulating fluidized bed pilot scale unit. Three different MgO materials were tested at different catalyst to biomass ratios in order to validate the findings of the lab scale testing. For comparison purposes, a commercially available fresh ZSM-5 catalyst was tested as well. In addition, the MgO catalytic materials were characterized before and after use in the pilot plant unit. This allowed for the evaluation of the effect that the process has on the catalyst and gave valuable insight of how it deactivates with time, especially when compared to the acidic ZSM-5 catalyst. Pilot scale validation confirmed the findings of the bench scale work regarding product yields and the effect that the MgO activity had on the efficiency of the process. Finally, 2DGC-TOFMS of the received bio-oils allowed for their detailed characterization and the validation of the deoxygenation mechanisms that differ in basic catalytic biomass pyrolysis.

2. Experimental

2.1. Materials and catalyst preparation

Three MgO catalysts, derived from natural magnesite, were tested in biomass fast pyrolysis on the pilot scale circulating fluidized bed reactor. The selection of the MgO samples was based on our previous work, which had investigated their performance, mechanisms and effects of their physicochemical properties. More details about the samples can be found in this publication [24].

In addition, a commercially available ZSM-5 catalyst was also tested in order to compare the product yields and selectivities, the deoxygenation mechanisms and the bio-oil qualities between acidic and basic catalytic upgrading. The ZSM-5 based catalyst was an industrial ZSM-5 based formulation that consisted of 30% crystalline zeolite diluted in a silica-alumina matrix.

The biomass used in the current study was a commercial lignocellulosic biomass (Lignocel HBS 150–500) originating from beech wood with elemental analysis of 45.98 wt. % carbon, 6.39 wt. % hydrogen, 46.28 wt. % oxygen, 0.66 wt. % ash. The alkali metals found in the ash of Lignocel sawdust have concentrations of 130 mg/kg Na, 452 mg/kg K, 365 mg/kg Mg, 120 mg/kg Fe and 1620 mg/kg Ca on dry biomass basis.

2.2. Characterization of MgO and ZSM-5 catalysts

The MgO samples were characterized by X-Ray Diffraction (XRD) to identify the crystal structure, Inductively Coupled Plasma - Atomic Emission Spectrometry (ICP-AES) to determine the chemical composition, N_2 adsorption-desorption to determine the surface area (BET method), total pore volume at P/Po = 0.99, micropore volume (t-plot method), and pore size distribution (BJH method), Scanning Electron Microscopy (SEM) to study the particle morphology and finally, Temperature Programmed Desorption of CO_2 (TPD − CO_2) to determine the basic properties of the MgO catalysts. The acidity of the ZSM-5 catalyst was determined by Fourier Transform Infrared Spectroscopy, combined with *in situ* adsorption of pyridine. More details on the equipment and analytical protocols used have been previously reported [6,24].

2.3. Catalytic pyrolysis tests

The recirculating fluidized bed pilot plant unit used in this work has been described elsewhere [25,26] and is presented in Fig. 1.

In short, the biomass was fed from the feed hopper to the hot reaction section using a screw feeder where it was mixed with the solid heat carrier (catalyst), which was loaded in the Catalyst Regenerator. The Catalyst Regenerator was a fluid bed reactor aiming to burn off the coke that was deposited on the catalyst and provided the required heat for the pyrolysis. The reactor consisted of a mixing zone vessel and the

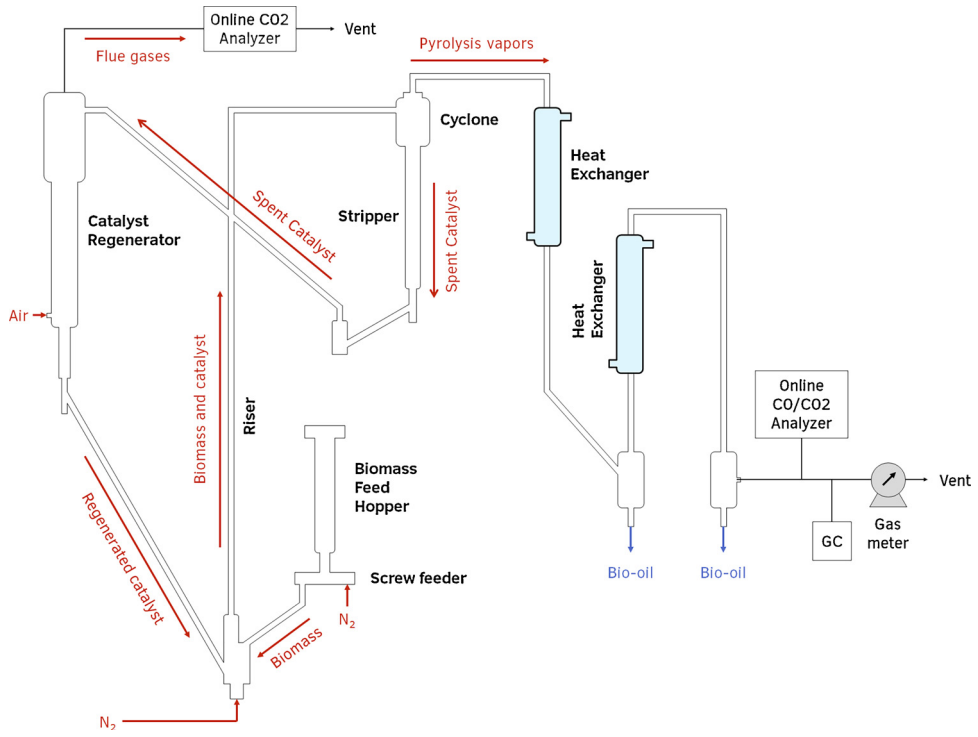

Fig. 1. Schematic diagram of the circulating fluidized bed biomass pyrolysis pilot plant.

riser. Once mixed, biomass, catalyst particles and bio-oil vapors were transported out of the mixing zone and into the riser where the pyrolysis reactions continued to take place. The mixture then entered the cyclonic head of the stripper tangentially, where bio-oil vapors and catalyst particles were separated. The spent catalyst was recirculated back to the regenerator to burn off the coke via a liftline. The bio-oil vapors entered the product recovery system, which encompassed a number of vessels and heat exchangers that recovered the produced bio-oil. The volume of the non-condensable cracked gases and the flue gases at the exit of the regenerator were measured via two wet test meters. The composition of the gaseous streams was determined by gas chromatography In addition, two Servomex 1440 infrared gas analyzers were used to continuously measure CO and CO_2 concentration in the non-condensable pyrolysis gases and CO_2 concentration in the flue gases at the exit of the regenerator. In contrast to our previous work that was conducted on a lab scale fixed bed reactor where only ~1 g of catalyst and biomass was sufficient, in this work an inventory of ~12 kgs of catalyst and ~ 1.5 kgs of biomass per run was necessary for the operation of the unit. The circulating fluidised bed process is a proven commercial refinery technology for the cracking of heavy petroleum feeds and the data obtained in this work can be considered as representative of the performance of a commercial biomass fast pyrolysis unit, operating under similar conditions.

2.4. Products analysis and characterization

Water content in the bio-oil was determined by Karl-Fischer titration in a Metrohm Titrino 795 K F titrator, according to ASTM E203-08. Elemental composition (carbon and hydrogen) was measured using a LECO-628 CHN elemental analyzer, according to ASTM D5291. Oxygen content was determined by difference. Micro carbon residue was determined according to ASTM D-4530. Total acid number was measured with a 751 Titrino Metrohm analyzer. Gaseous products were analyzed in a HP 5890 Series II gas chromatograph equipped with four columns (Precolumn: OV-101; Columns: Porapak N. Molecular Sieve 5 A and Rt-Qplot 30 m × 0.53 mm ID) and two detectors (TCD and FID).

Quantitative analysis of the compounds in the bio-oil samples was performed by means of two-dimensional gas chromatography coupled with time-of-flight mass spectrometry (2DGC-ToFMS). The 2DGC analytical system was an Agilent 7890 A GC with injector Agilent7683B series (Agilent Technologies, PaloAlto, CA, USA) connected to a Pegasus 4D time-of-flight mass spectrometer from Leco Instruments (St. Joseph, MI, USA). The quantitative analysis was carried out according to the internal calibration method and phenol-d6 was used as the internal standard. Details on the equipment and quantification method can be found in previous communications [27,28].

3. Results and discussion

3.1. Effect of catalysts on product yields

3.1.1. Catalyst properties

Tables 1 and 2 present the properties of the three MgO catalysts before and after use in the pilot unit while the N_2 adsorption-desorption isotherms of the MgO catalysts and the respective pore size distribution curves are shown in Fig. S1 of the Supplementary material. TPD − CO_2

Table 1
Surface areas, pore volume and pore diameters of MgO samples before and after use in the pilot unit.

Catalyst[a]	BET surface area[b] (m^2/g)	Total pore volume[c] (cc/g)	Mean pore diameter[d] (nm)
MgO-20-0 h	19.6	0.179	21.2
MgO-20-25 h	9.6	0.125	47.3
MgO-25-0 h	25.2	0.248	26.1
MgO-25-15 h	14.5	0.161	44.4
MgO-40-0 h	44.4	0.286	23.1
MgO-40-22 h	23.1	0.265	45.4
MgO-40-30 h	22.3	0.218	38.9

[a] The last number in each catalyst name indicates the hours (h) of biomass pyrolysis in the pilot scale unit.
[b] BET area from N_2 sorption at −196 °C, multi-point BET method.
[c] at P/Po = 0.99.
[d] from BJH pore size distribution curves.

Table 2
Basicity (μmol CO_2/g) of MgO catalysts before and after use in the pilot unit.

Catalyst	Basicity (μmol CO_2/g)	Iw/s[a]	Weak/ medium sites (μmol/g)	Tmax of weak/ medium sites (°C)	Strong sites (μmol/g)	Tmax of strong sites (°C)	Crystal size (nm)[b]
MgO-20	85.9	3.6	67.1	246	18.8	526	35.3
MgO-20-25 h	31.7	1.1	16.8	187	14.9	511	49.4
MgO-25	121.8	3.6	95.1	252	26.7	532	28.5
MgO-25-15 h	37.4	2.9	28.0	191	9.4	500	44.9
MgO-40	138.9	2.4	97.6	270	41.3	526	23.8
MgO-40-30 h	85.4	2.5	61.2	212	24.2	517	29.8

[a] Ratio of weak to strong basicity and.
[b] Calculated from Scherrer equation using XRD data of peak 2θ = 42.9°.

curves of the MgO catalysts before and after pilot plant testing are also shown in Figure S2. The first two digits in the MgO catalyst name (i.e. MgO-20-25 h) represent and approximation of their original surface area (as fresh catalysts), while the last digits represent the time-on-stream in the pilot plant unit. Where no time-on-stream is indicated, a fresh catalyst sample is implied. Details about the loss of activity attributed to loss of basicity and surface area are discussed in Section 3.3. The fresh ZSM-5 catalyst that was tested for comparison purposes, had a total surface area of 148 m^2/g, of which 117.5 m^2/g were attributed to the zeolite and 30.5 m^2/g were attributed to the matrix. In addition, the Brønsted and Lewis acid sites content of the zeolite was 36.0 and 20.0 μmol Pyr/g respectively. The catalysts' properties and how they were affected by consecutive runs in the pilot scale are discussed in detail in Section 3.3.

3.1.2. Effect of catalyst to biomass ratio on product yields

One of the main process parameters of the recirculating fluidized bed technology that can significantly affect product yields and quality is the catalyst-to-feed ratio. In recirculating fluidized bed technology which is a continuous process and fresh catalyst is constantly introduced in the reactor, the catalyst to feed ratio is defined as the catalyst circulation flow in kg/hr to the feed (in this case biomass) introduction flow in kg/hr, as in the case of fluid catalytic cracking technology (FCC) employed in the refinery industry. Tuning of the catalyst to biomass ratio (Cat/Bm) is a means of controlling the bio-oil's properties, such as oxygen content, viscosity, density, hydrocarbon concentration and HHV, among others. In our previous work, it was shown that by varying the Cat/Bm for a ZSM-5 catalyst it was possible to increase the quality of the bio-oil (by decrease of its oxygen content) at the expense of the bio-oil yield [26]. Typically increasing the Cat/Bm ratio increases the desirable reactions, in this case deoxygenation carbon coupling reactions as noted in the following paragraphs, resulting in better quality bio-oils (less O_2 content) to the detriment of bio-oil yield (increased carbon losses towards coke and non condensable gases). In the catalytic fast pyrolysis tests of the present work, two distinct bio-oil phases were produced and separated easily. The bottom dark layer (labeled organic phase) typically had low water content (3–10%), while the top light layer (labeled aqueous phase) consisted mostly of water (70–90%) and water-soluble oxygenated compounds, such as low MW organic acids, phenols, ketones and aldehydes. Since the organic phase of the bio-oil found in the dark bottom layer is the one typically retrieved as bio-oil and of main interest, we will refer to this as dry bio-oil yield, while dry bio-oil oxygen content will also refer to the bio-oil recovered in this phase.

Fig. 2 presents the effect of Cat/Bm ratio on the pyrolysis product yields for the ZSM-5 and MgO catalysts used in the present work. The catalysts presented in Fig. 2 had 0 h of previous run time and they were therefore considered fresh catalysts. In agreement with what has been reported so far in the literature, an increase of the Cat/Bm ratio led to a decrease of the dry bio-oil yield and an increase of the char and coke yield, while total H_2O yield remained more or less unaffected in all cases. In the case of the MgO catalysts, CO_2 increased with increasing Cat/Bm ratio, while CO yield was unaffected. These data are in accordance with the increased yields of CO_2 obtained in the lab-scale experiments with the MgO catalysts [24]. In the case of the ZSM-5 catalyst, CO_2 yield was not found to increase with Cat/Bm ratio, while CO was slightly increased, also in agreement with the lab-scale experiments [24].

In all plots in Fig. 2, it is clear that the MgO catalyst with the higher surface area (MgO-40) was the most reactive amongst the MgOs, being also more reactive than the acidic ZSM-5 zeolite in terms of conversion of the organic (dry) bio-oil. The deoxygenation activity of these two catalysts was similar but for all the other products they exhibited different behavior. In general, the MgO-40 induced higher CO_2 and solids (char and coke) formation and lower CO and water, while the ZSM-5 favored the production of water and CO. The activity of all the catalysts is discussed in detail in the following paragraphs.

3.1.3. Acidic vs basic catalytic upgrading

Solid products yield was markedly higher in the case of the MgO samples compared to ZSM-5. In contrast to the strongly acidic microporous ZSM-5, the MgO samples possessed no acidic active sites, but instead had basic active sites located on meso/macropores. As in our previous work [24], the high solid product yields were attributed to coke formation in the mesopores, which allowed intermediate fragments produced from biomass pyrolysis to condensate due to thermal effects and possibly via basic catalytic action. On the other hand, in the case of the ZSM-5 catalyst, coke production was driven by condensation of the initially formed aromatic hydrocarbons towards polycyclic aromatic hydrocarbons (PAHs), which polymerized further to form extremely stable coke of aromatic nature [29,30]. Dies alder and aldol condensation reactions, the latter typically enhanced by basic catalysis, are also potential pathways for the condensation of small oxygenates towards larger molecules that were further converted to coke [31,32]. In our previous work temperature programmed oxidation (TPO) and thermogravimetric analysis (TGA) of the coked MgO and ZSM-5 samples revealed significant differences in the nature of carbonaceuous deposits on each catalyst. The coke on MgO was more oxygenated and was oxidized at much lower temperature (371 °C - temperature of maximum CO_2 evolution) when compared to the ZSM-5 produced coke (420 °C for an industrially formulated catalyst containing 30% ZSM-5 zeolite and 482 °C for a pure ZSM-5 zeolite). Thus, a "softer" and more oxygenated coke was suggested to be formed on MgO, compared to the more stable and "hard" coke produced on ZSM-5 [24].

The physicochemical characteristic of the MgO materials that determined their catalytic activity was mainly their surface area, especially if taken into account that their basicity was in part proportional to it (Table 2). The MgO-40 sample was the most active, producing less bio-oil and higher solid product and CO_2 yields compared to the other MgOs. H_2O and CO yields were more or less unaffected by both the surface area and the Cat/Bm ratio, therefore the overall activity when using a basic catalyst had no impact on these deoxygenation products. This is in complete contrast to the behavior of the acidic ZSM-5 catalyst. Both H_2O and CO were the main deoxygenation products of ZSM-5, as

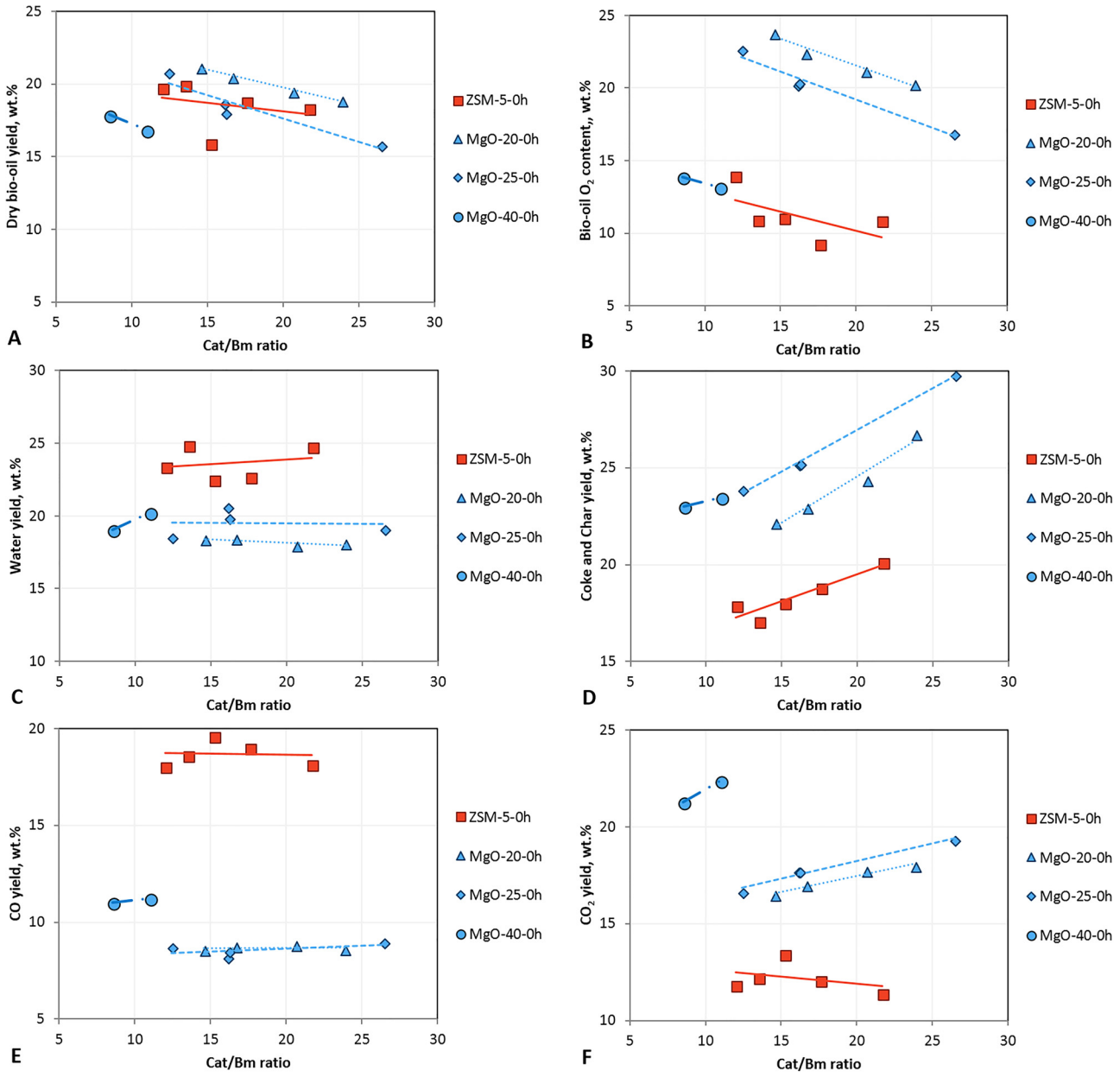

Fig. 2. Effect of Cat/Bm ratio on the a) dry bio-oil yield, b) dry bio-oil oxygen content, c) H_2O yield, d) solid products yield, e) CO and f) CO_2 yields on dry ash-free biomass basis.

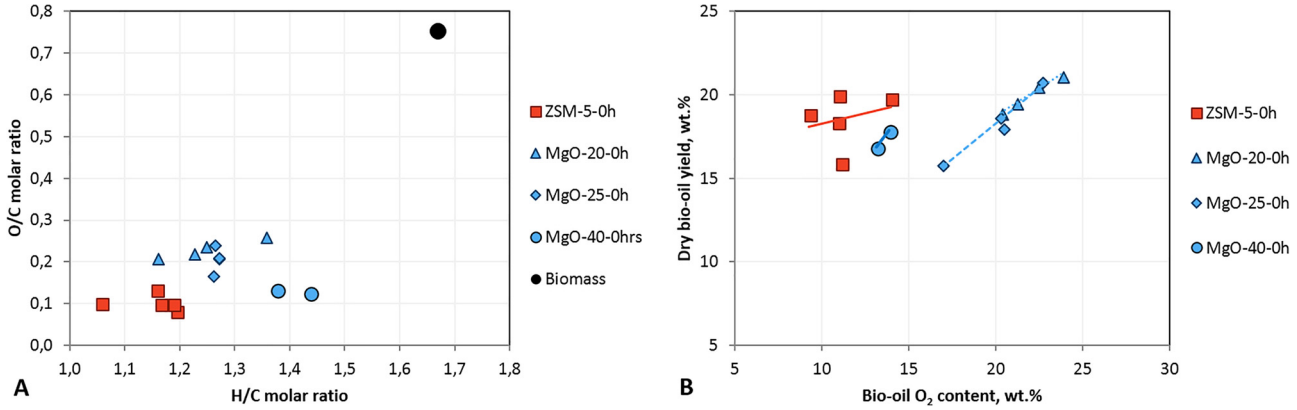

Fig. 3. (a) Van Krevelen diagram for bio-oils produced with MgO and ZSM-5 catalysts, (b) dry bio-oil yield vs bio-oil O_2 content.

Table 3
Elemental analysis and characterization of MgO and ZSM-5 bio-oils.

Catalyst	ZSM-5	MgO-20	MgO-25	MgO-40
Cat/Bm	15.2	14.6	16.2	11.0
Organic phase				
H_2O (wt.%)	3.4	7.6	9.2	3.3
TAN (mg KOH/gr)[a]	11.6	48.6	60.6	13.0
MCR (%)[b]	10.8	16.4	17.8	11.1
Elemental analysis (dry basis)				
C (wt.%)	81.7	68.4	72.0	77.5
H (wt.%)	7.2	7.7	7.6	9.3
O (wt.%)	11.1	23.8	20.4	13.2
Aqueous phase				
H_2O (wt.%)	89.6	68.8	76.9	91.6
TAN (mg KOH/gr)	38.5	79.0	61.3	20.1
Elemental analysis (dry basis)				
C (wt.%)	49.5	49.5	51.9	51.6
H (wt.%)	6.0	12.0	12.4	9.8
O (wt.%)	44.5	38.5	35.7	38.6

[a] Total Acid Number and.
[b] Micro Carbon Residue.

clearly depicted in Figs. 2c and 2e. The ZSM-5 catalyst enhanced decarbonylation, dehydration and aromatization reactions [25], all of which led to the formation of CO and H_2O as the main deoxygenation products. On the other hand, MgO enhanced ketonization and aldol condensation reactions, which led to the formation of mainly CO_2 and H_2O. CO_2 formation is a much more preferable deoxygenation route compared to CO, since only one atom (12 g/mol) of C is sacrificed to remove two atoms (32 g/mol) of O. Moreover, H_2O production was significantly decreased, around 4 wt.% on dry biomass basis when comparing the two most active catalysts, ZSM-5 and MgO-40. Even though the reduction in H_2O formation denote a lesser degree of deoxygenation, it also implies that more hydrogen was conserved and recovered in the bio-oil product, leading to better fuel properties. This is demonstrated in Fig. 3, where a Van Krevelen diagram for the bio-oil samples of this work is presented along with a plot of the bio-oil yield versus its O_2 content which is indicative of its quality. H/C ratio was clearly higher for all MgO bio-oils when compared to ZSM-5. This can also be seen in Table 3, where the elemental composition of the bio-oil samples is presented.

Fig. 4 presents the oxygen and carbon distribution in the final products as a percentage of the initial oxygen and carbon input from the biomass feed. By comparing the ZSM-5 with the most active MgO-40 material, the gain in deoxygenation via basic catalysis becomes apparent. In the case of basic catalysis, the amount of oxygen removed as CO decreased from 24.6 to 10.6 wt.% on initial oxygen input, and the amount of carbon removed as CO was reduced from 17.5 to 6.8 wt.% on initial carbon input. Overall, a difference of 14 wt.% and 10.7 wt.% for oxygen and carbon, respectively, was observed. On the other hand, the amount of oxygen removed as CO_2 increased from 19.5 wt.% (ZSM-5) to 33.2 wt.% (MgO-40), with a corresponding increase in carbon loss from 6.9 wt.% to 10.6 wt.% (overall differences of 13.8 wt.% and 3.7 wt.% for oxygen and carbon, respectively). Therefore, deoxygenation with the MgO-40 catalyst via CO_2 formation rather than CO, conserved 7 wt.% of the carbon input.

It is also apparent from Fig. 4 that the main disadvantage of the MgO materials was the formation of coke, which resulted in up to 52% carbon lost towards the solid byproduct. On the other hand, the ZSM-5 catalyst exhibited carbon losses of only about 39% due to its narrow channel microporous structure that inhibits the formation of large molecules and condensates. A potential strategy for increasing catalyst efficiency in the catalytic fast pyrolysis of biomass could be the development of basic catalysts with optimized particle morphology and porosity or the combination of acidic-basic sites on a microporous zeolite such as ZSM-5 [33,34].

3.2. Effect of catalysts' properties on bio-oil quality

3.2.1. Elemental analysis and standard characterization of bio-oils

Table 3 presents the elemental analysis of the bio-oils retrieved in the organic and aqueous phases at Cat/Bm ratio around 15. As already mentioned, the hydrogen content of the bio-oils produced with the MgO catalysts was higher compared to the one produced with the ZSM-5 catalyst, due to less extensive dehydration reactions (Section 3.1.3).

As expected, the ZSM-5 and the MgO-40 catalysts, which were the most active ones in this work, produced bio-oils with the lowest oxygen content and the lower TAN. In general, MgO bio-oils had higher TANs compared to the bio-oil produced with ZSM-5. The elemental composition of the dry aqueous phase fraction was harder to determine due to the very high H_2O content, however similar trends were noted for the TAN and the water content. Finally, MCR, which is an indication of residual high molecular mass compounds and solids in the liquids, was lowest with the most active catalysts, ZSM-5 and MgO-40.

3.2.2. Advanced characterization of bio-oils

2DGC-TOFMS was used as an advanced method of characterization in order to determine the chemical composition of the produced bio-oils and to quantify the most abundant compounds. Table 4 presents quantitative data for the samples produced with the ZSM-5 and MgO-40 catalysts. The chemical compounds detected and quantified were grouped in order to draw conclusions about the performance of the catalysts.

As it can be seen in Table 4, the ZSM-5 catalyst produced aromatic hydrocarbons (AR) selectively (21.3 wt.% on wet organic phase bio-oil). The MgO-40 on the other hand yielded almost no AR due to its basicity and in contrast, the production of ketones was increased.

Table 5 presents a more detailed view the most abundant compounds detected by 2DGC-TOFMS. In the case of the ZSM-5, mostly aromatic compounds (either mono-aromatics and naphthalenes) and phenolics were detected. On the other hand, the MgO-40 yielded ketones and more specifically cyclo-pentenones. The mechanisms that lead to the formation of aromatic products in the case of the ZSM-5 are well known and have been thoroughly investigated in the literature [35–39]. Ketone production from the MgO-40 is attributed to ketonization and aldol condensation reactions of low molecular weight ketones, aldehydes and organic acids commonly found in biomass pyrolysis vapors [40–42]. Acidic zeolites such as ZSM-5 typically crack this type of molecules towards even lighter products, such as CO, CO_2 and light gaseous hydrocarbons. However, in the case of the basic MgO materials, these compounds were upgraded via carbon coupling reactions. Some representative reactions are demonstrated in Schemes 1 and 4.

Scheme 1 demonstrates a ketonization reaction of one of the most abundant organic acids in bio-oil, acetic acid (AA). Two molecules of AA condense to produce acetone along with CO_2 and H_2O as by-products. Pham et al. [43] have described this mechanism based on the β-keto acid intermediate thoroughly. Pulido et al. [44] have described this ketonic decarboxylation route in detail on ZrO_2 catalyst. They proposed two different routes based on the mechanism suggested by Rand et al. [45]. A reaction pathway with the formation of a β-keto acid intermediate was considered, as well as a concerted mechanism, involving simultaneous carbon–carbon bond formation and carbon dioxide elimination. They found that the β-keto acid route was kinetically favored and proposed this mechanism as the predominant one. Scheme 1 demonstrates this mechanism over an MgO catalyst.

The acetone molecules may condensate further via an aldol condensation reaction as shown in Scheme 2. In aldol condensation reactions, catalyzed by basic catalysts, an enolate formed from an aldehyde or ketone reacts with a carbonyl compound to form a β-hydroxyaldehyde or a β-hydroxyketone [46]. Further dehydration leads to the production of an α,β-unsaturated carbonyl compound such as the one presented in Scheme 3, which is an example of an MgO-catalyzed

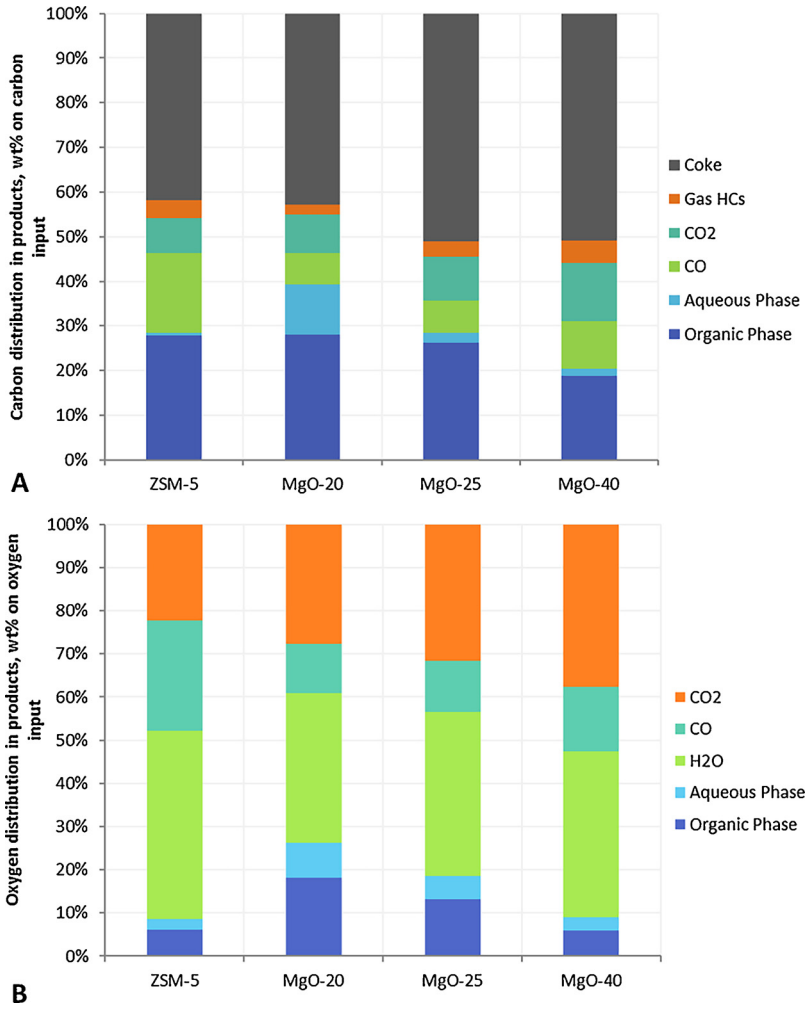

Fig. 4. (a) Biomass oxygen distribution in pyrolysis products, (b) biomass carbon distribution in pyrolysis products, for MgO and ZSM-5 catalysts.

Table 4
Grouping of chemical compounds quantified in bio-oils via 2DGC-TOFMS internal standard analysis, percentages are on the organic phase of the bio-oil, including water.

Group	ZSM-5 Total, % w/w	MgO-40 Total, % w/w
Aromatic hydrocarbons	21.30	1.16
Aliphatic hydrocarbons	1.22	2.35
Phenols	19.88	4.56
Furans	1.78	1.33
Acids	0.00	0.00
Esters	0.24	0.00
Alcohols	0.17	0.02
Ethers	0.07	0.07
Aldehydes	1.10	1.53
Ketones	2.14	9.27
PAH	5.84	0.11
Sugars	0.00	0.00
Nitrogen compounds	0.03	0.00
Total	53.77	20.39

aldol condensation reaction of two molecules of acetaldehyde producing but-2-enal. Biomass pyrolysis vapors contain such low MW aldehydes (C1-C5), which can participate in a multitude of condensation reactions typically producing C5-C8 condensation products. Scheme 4 demonstrates an intramolecular aldol condensation reaction. It requires a dicarbonyl compound and usually results in 5 or 6 member rings that have been found to be more stable products due to almost zero ring strain [47]. The low MW acids, ketones and aldehydes with 1 to 4 carbon atoms can participate in the above reactions in a number of combinations, yielding mostly 5- and 6-member ring cycloketones, H_2O and CO_2. This is evident in Table 5 where it can be seen that cyclopentenone, cyclohexenone and their derivatives were clearly the main products from the catalytic pyrolysis of biomass with basic MgO catalysts.

3.3. MgO catalyst deactivation over time

A major issue with the catalytic pyrolysis of biomass is the fast catalyst deactivation that has been documented for commercial catalysts such as ZSM-5 [17]. There are two types of catalyst deactivation that may occur during biomass pyrolysis. One is the deactivation due to coking and blockage of the surface area and catalyst pores. This is easily reversible by burning off the coke and regenerating the catalyst continuously, as it is done in industrial practice. The second type of deactivation involves both hydrothermal deactivation, due to contact with water vapor at high temperatures, as well as poisoning from biomass metals. The water vapor can originate from the moisture in the biomass feedstock, from dehydration reactions that take place during the thermal decomposition of the biomass and the catalytic upgrading of the pyrolysis vapors, as well as from char and coke oxidation reactions during the catalyst regeneration stage. Water vapor dealuminates the zeolitic framework, especially in the regeneration vessel (temperatures of 650 °C or higher), which results in the reduction of both the strength and density of the acid sites [17].

Table 5
20 most abundant compounds quantified via 2DGC-TOFMS analysis in ZSM-5-0 h and MgO-40-0 h bio-oils on wet organic phase of bio-oil.

ZSM-5 *Compound*	*% w/w*	MgO-40 *Compound*	*% w/w*
p-Xylene	7.00	2-Cyclopenten-1-one, 2-methyl-	1.43
Phenol, 3-methyl-	4.14	Phenol, 2-methyl-	0.66
Phenol	3.35	2-Cyclopenten-1-one, 2,3-dimethyl-	0.62
Naphthalene	2.35	2-Cyclopenten-1-one, 3,4-dimethyl-	0.62
Phenol, 3-methyl-	2.25	Benzaldehyde	0.61
Naphthalene, 1,7-dimethyl-	2.06	2-Cyclopenten-1-one	0.60
Toluene	1.97	Phenol	0.55
Phenol, 2,3-dimethyl-	1.65	Furfural	0.55
1H-Indene, 1,3-dimethyl-	1.23	Phenol, 3-methyl-	0.54
Ethylbenzene	1.11	Phenol, 2,5-dimethyl-	0.43
Benzene, 1,2,3-trimethyl-	1.07	2-Cyclopenten-1-one, 2,3,4-trimethyl-	0.42
1,2-Benzenediol	1.02	2-Cyclopenten-1-one, 3-methyl-	0.33
2-Propenal, 3-phenyl-	1.00	3-Cyclohexene-1-acetaldehyde, 4-dimethyl-	0.32
Benzofuran, 2-methyl-	0.99	1,2-Dipropylcyclopropene	0.27
Benzene, 1-ethynyl-2-methyl-	0.94	2-Cyclopenten-1-one, 3,4-dimethyl-	0.26
Benzene, 1,3-dimethyl-	0.92	2-Cyclohexen-1-one	0.24
Benzene, 1-ethyl-4-methyl-	0.90	1.4-Cyclohexadiene, 1-methyl-	0.23
1H-Indene, 2,3-dihydro-4-methyl-	0.83	2-Butanone	0.21
Benzene, 1-ethenyl-2-methyl-	0.83	2-Cyclopenten-1-one, 3,4-dimethyl-	0.21
Phenol, 2,6-dimethoxy-	0.73	2-Cyclopenten-1-one, 2,3-dimethyl-	0.21
1.2-Benzenediol, 3-methoxy-	0.52		
Total $_{\text{Top 20 compounds}}$ (% w/w)	36.33	Total $_{\text{Top 20 compounds}}$ (% w/w)	9.29
Total (% w/w)	53.77	Total (% w/w)	20.39

Poisoning of acidic zeolites can occur due to alkali and alkaline earth metals commonly found in biomass. Mullen and Boateng [48] found that K deposited on the catalyst more rapidly, although the deposition rate declined with increased biomass loading. Ca deposited less rapidly but the deposition rate did not decline with increased biomass loading and was nearly linear. Mg, Cu and Fe also deposited almost linearly. The regenerated catalyst was not as effective in the conversion of oxygenates to aromatic hydrocarbons as the fresh catalyst. Paasikallio et al. [49] investigated the deactivation of an HZSM-5 catalyst during a four day catalytic fast pyrolysis run of pine wood. Despite a clear trend that showed oxygen increase in the bio-oil over the course of the run, that increase was small (from 22.4 to 23.7 wt%) and the catalyst retained its activity for the period that was studied. However, poisoning of the acid sites, which appear to attract the basic alkalis of biomass, can significantly reduce the catalyst's life, especially since alkali metals concentration in biomass is in the order of 0.3 wt.% and higher. Work from our group [17] has shown that K and Na deposit very selectively on the catalyst surface while Ca and Mg also deposit albeit at a lower rate. However, since they have higher concentrations in the biomass ash they are also responsible for significant deactivation of the catalyst.

The deactivation of basic catalysts has not been documented in the literature, especially in pilot scale testing which can approximate real life industrial processes. The basic sites are expected to be unaffected by alkali deposition in contrast to what has been documented for acidic zeolites. To investigate the deactivation of the MgO catalysts, consecutive runs were done in pilot scale. The MgO-20 catalyst was used for the catalytic pyrolysis of a total of 10 kg of biomass for a total run time of 25 h (MgO-20-25 h). The MgO-25 catalyst was used for the catalytic pyrolysis of 6 kg of biomass for a total run time of 15 h (MgO-25-15 h). Finally, the MgO-40 catalyst, which was the most active and most promising one was studied in three stages. In the first stage, it was used for the catalytic pyrolysis of 5 kg of biomass for a total run time of 10 h (MgO-40-10 h). In this initial stage of runs, a rapid loss of activity was observed as can be derived from the deteriorated textural and basic properties (Tables 1 and 2) and the reduced deoxygenation of the bio-oil (Fig. 5). It was then reintroduced in the pilot unit for two additional campaigns of runs. The second campaign lasted 12 h, after which the

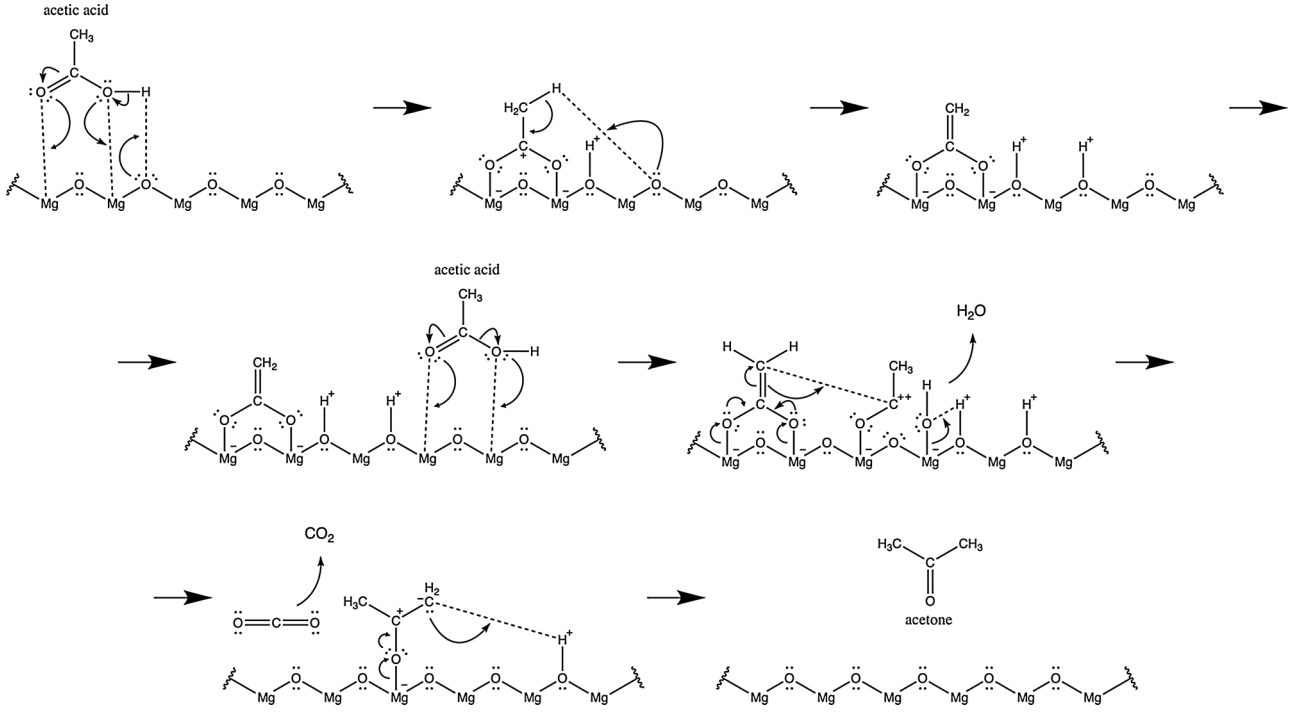

Scheme 1. Ketonization of acetic acid over MgO catalysts for the formation of acetone, with CO_2 and H_2O as byproducts.

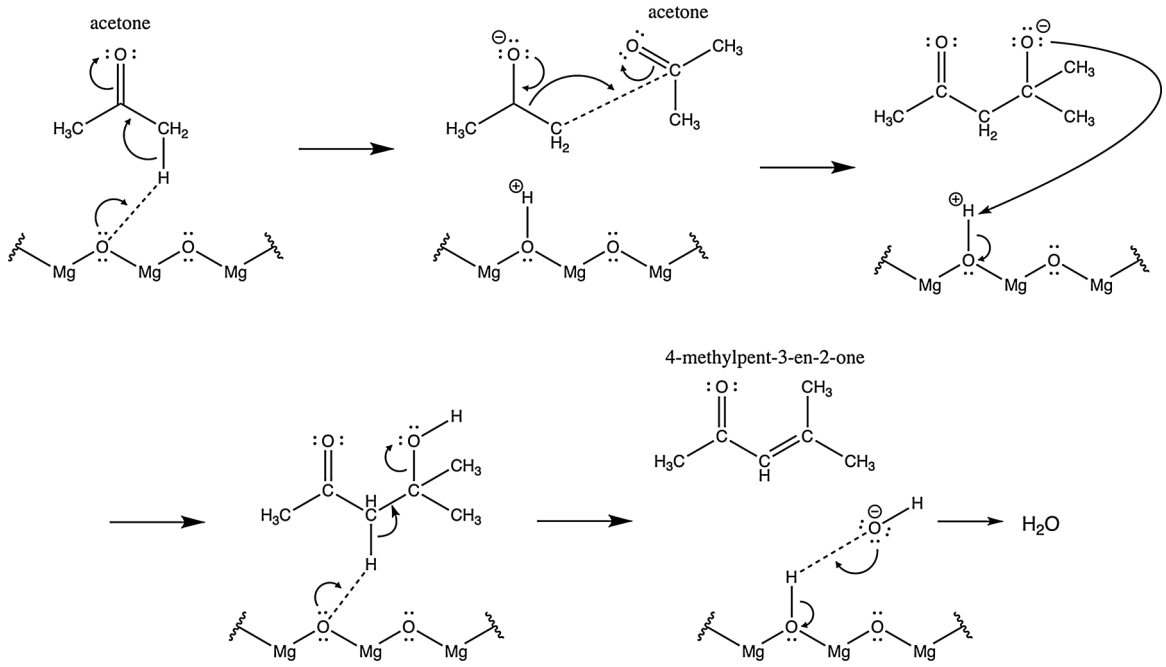

Scheme 2. Aldol condensation of acetone over MgO catalysts for the formation of 4-methylpent-3-en-2-one, with H_2O as byproduct.

sample was named MgO-40-22 h. The third campaign lasted for another 8 h and yielded the final sample named MgO-40-30 h.

Fresh catalysts tend to lose a significant portion of their activity in the first part of their lifetime showing extremely high rates of deactivation. This is verified in the case of the MgO-40 catalyst. Rapid initial deactivation was observed, in which most of the activity loss occurred during the first 5 h of the catalytic pyrolysis runs. Afterwards, the activity of the catalyst reached a plateau and remained stable throughout the following sets of runs.

Tables 1 and 2 present the main physicochemical properties of the catalysts before and after use in the pilot scale unit while N_2 adsorption-desorption isotherms of the MgO catalysts and their respective pore size distribution curves are presented in Figure S1. The adsorption isotherms of all the MgO catalysts are of type II (IUPAC classification), showing relatively narrow hysteresis loops, typical of non-porous materials or materials with high textural porosity originating from inter-crystal/particle voids at the meso/macroporous scale. The measured BET surface area (20–44 m^2/g) of the fresh catalysts was attributed mainly to inter-crystal/particle meso/macropores with average diameters of ca. 21–26 nm (Table 1). As shown in our previous work [24] the decrease of crystal size is accompanied by increase of surface area due to the higher external surface and/or inter-particle porosity of smaller (nano) crystals. With regard to the used catalysts, there was significant change in the porosity characteristics after some time-on-stream. At the same time, an increase in the crystal size was noticed for all the MgO catalysts possibly due to a partial crystal sintering during

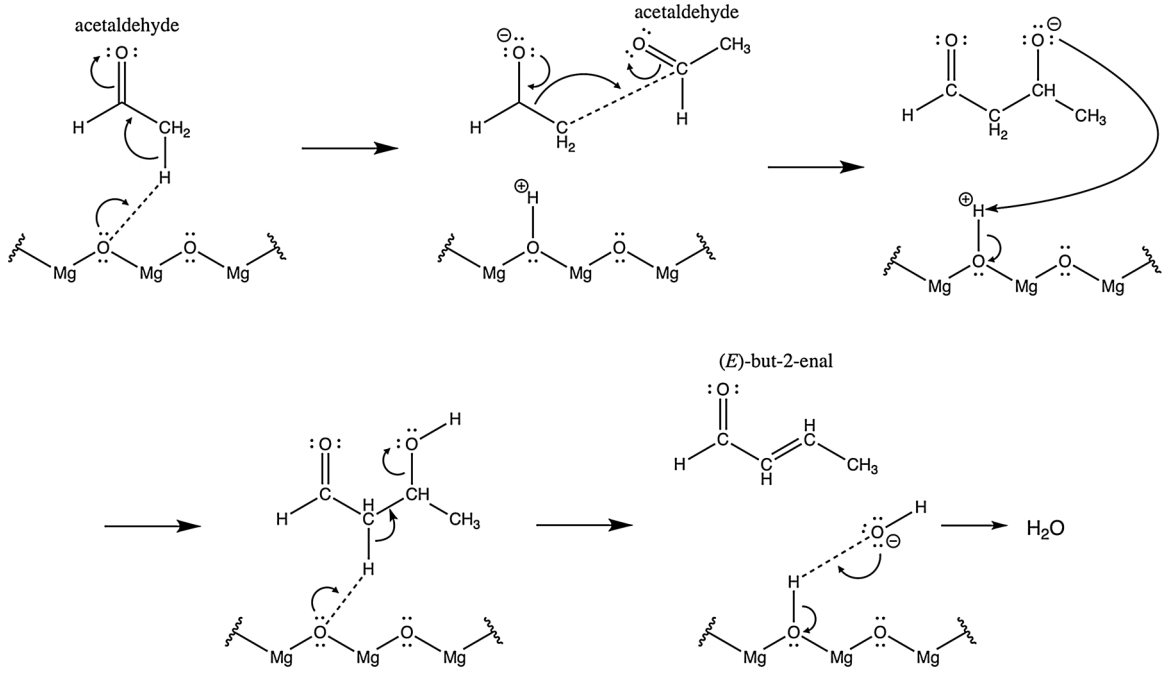

Scheme 3. Aldol condensation of acetaldehyde over MgO catalysts for the formation of (E)-but-2-enal, with H_2O as byproduct.

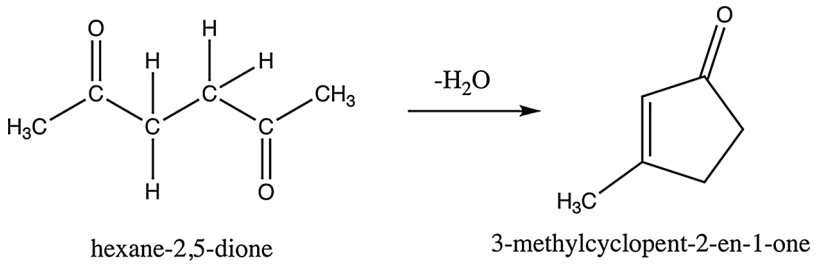

Scheme 4. Intramolecular aldol condensation of hexane-2,5-dione for the formation of 3-methylcyclopent-2-en-1-one, with H_2O as byproduct.

time-on-stream reaction and regeneration cycles. Thus, the lower surface area of the used MgO-20, MgO-25 and MgO-40 samples by 51.2%, 42.5% and 49.8% respectively when compared to the corresponding fresh samples, can be attributed to the increase of the crystal size.

Since porosity and basicity are actually interrelated properties for the MgO catalysts, a decrease in basicity for the used samples was expected and verified after TPD − CO_2 experiments. The TPD − CO_2 curves are presented in Figure S2, while the total number of basic sites (total basicity), the number of weak/medium and strong basic sites, the ratio between them and the temperature maxima of the respective TPD − CO_2 peaks are shown in Table 2. The TPD − CO_2 curves of all MgO catalysts show similar behavior exhibiting two peaks; the first between 100 and 400 °C (with maxima in the range of 200–260 °C), attributed to weak/medium basic sites, and the second between 450 and 600 °C (with maxima in the range of 500–530 °C) attributed to strong basic sites. After time-on-stream, a decrease in basicity was noticed in all cases, mostly of the moderate strength sites (Figure S2). The smaller decrease was noticed for MgO-40 catalyst (38.5%) and this effect was only intense for the first test run since when comparing with the basicity of the used MgO-40 catalyst after 22 and 30 h on stream, very minimal loss of surface area and consecutively lower decrease in basicity was observed.

Moreover, the two campaign runs between 10–22 and 22–30 h time-on-stream gave very similar product yields and bio-oil quality (oxygen content), as it can be seen in Fig. 5.

The above data support the hypothesis that in the beginning of the MgO catalyst's life there is a significant deactivation before an equilibrium state is achieved, as is the case for commercial acidic zeolites. Loss of surface area and basicity can be attributed to the sintering of MgO crystallites, as suggested also above, caused by exposure at high temperatures in the regenerator during coke burnout (650 °C or higher). XRD analysis of the fresh and used samples showed a significant increase of the MgO crystal sizes. Table 2 shows an increase of crystal size in the cases of MgO-20 and MgO-25 of 40 and 57% respectively. The MgO-40 appeared to be far more stable with a total increase in crystal size of 25%, despite having a longer overall run time. It is noteworthy that even though both surface area and basicity were significantly reduced in the case of the MgO-20 and MgO-25, their actual catalytic performance was not that affected. The MgO-40 sample, which had the highest surface area amongst the MgO catalysts, was more significantly affected, as it can be seen in Fig. 5. The original fresh material had a surface area of 44 m^2/g and was quite active in producing bio-oil with low oxygen content. After 10 h time-on-stream, the surface area of the MgO-40 catalyst reduced to 23 m^2/g and correspondingly, the bio-oil produced was less deoxygenated. It is noteworthy however that

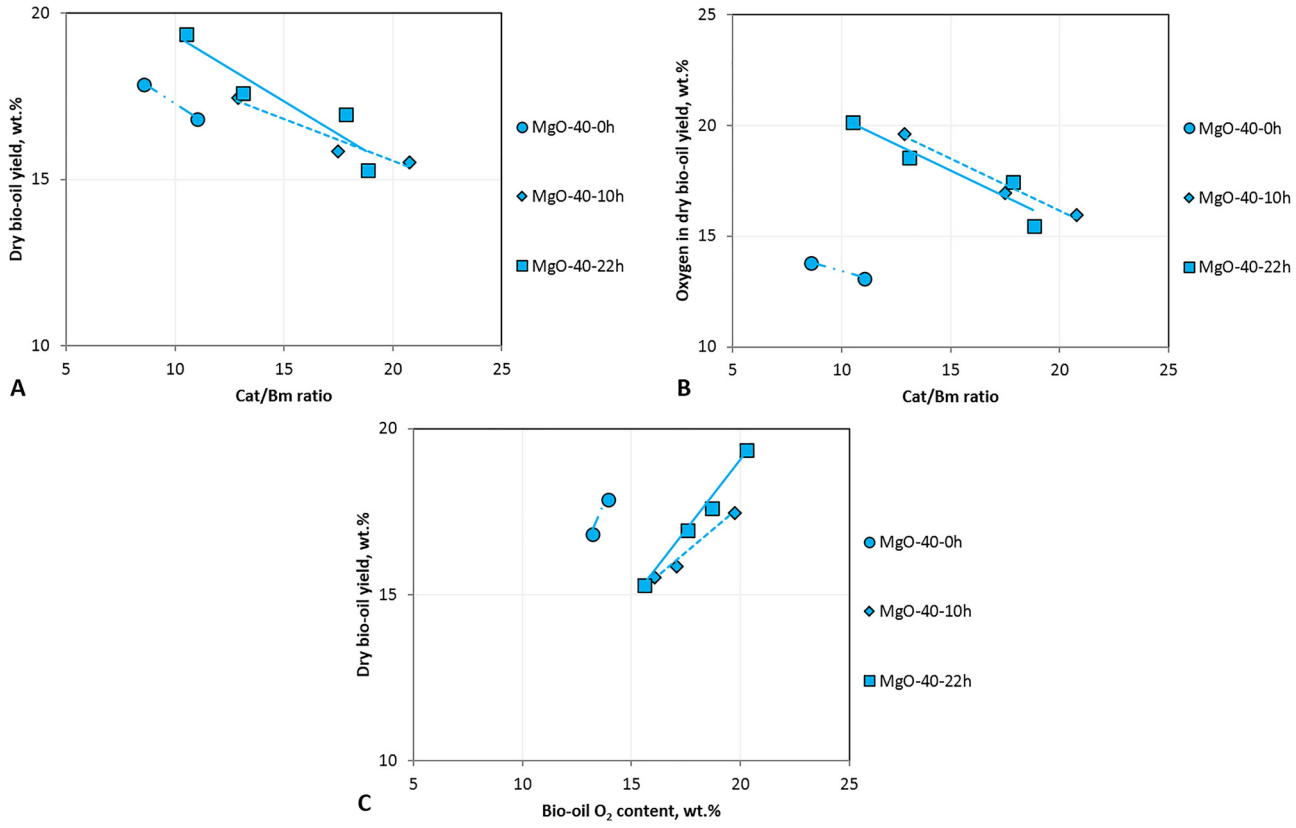

Fig. 5. (a) MgO-40 dry bio-oil yield and (b) dry bio-oil oxygen content as a function of Cat/Bm ratio at different run times and deactivation levels of the catalyst.

Table 6
Chemical composition of fresh and used MgO catalysts.

Catalyst	Chemical composition. wt.% (via ICP)							
	MgO	SiO_2[a]	CaO	Fe_2O_3	Al_2O_3	NiO	K_2O	NaO
MgO-20	89.87	7.35	2.18	0.14	0.38	0.078	0.0	0.0
MgO-20-25 h	92.52	5.05	2.16	0.19	0.00	0.084	0.0	0.0
MgO-25	97.16	1.49	1.21	0.04	0.04	0.052	0.0	0.0
MgO-25-15 h	95.23	3.30	1.35	0.06	0.00	0.056	0.0	0.0
MgO-40	87.86	10.12	1.73	0.21	0.00	0.076	0.0	0.0
MgO-40-30 h	88.14	9.08	1.86	0.82	0.00	0.105	0.0	0.0

[a] Nominal Si percentage value calculated by the abstraction of impurities and MgO percentage.

between 10 and 22 h time-on-stream, the performance of the catalyst was stabilized, indicating the stability of the material after the initial break-in period. Another observation was that there was significant increase in the pore size of all MgO catalysts after use in the pyrolysis pilot plant. This can also be attributed to crystal agglomeration, which led to the agglomeration of smaller mesopores and the generation of larger mesopores.

In summary, the MgO-40 sample proved to be quite resistant to sintering with time on stream, retaining higher surface area and basicity compared to the other two MgO catalysts, thus being a promising candidate for biomass fast pyrolysis continuous process. When compared to the deactivation of ZSM-5 zeolite, MgOs lose their initial activity due to loss of surface area and basicity, mostly associated with crystal size increase and sintering effects.

Elemental analysis of the fresh and used MgO samples is presented in Table 6. Interestingly, zero accumulation of K and Na was observed, even though both of these alkali metals tend to accumulate on acidic zeolites, as it has been shown in the literature by our own team, as well as other research groups [17,48]. In fact, unpublished data of used deactivated ZSM-5 catalyst retrieved from CPERI pilot plant indicate clearly a high deposition rate of K and Na, almost 100% and > 50% respectively, while Mg and Ca also deposit, albeit at a lower rate. This supports the hypothesis that metal accumulation is not a simple deposition mechanism of the metals on the surface and cavities of the catalyst; instead, it requires the presence of acid sites that attract and react with the alkalis locking them in place. The lack of these acid sites in the MgO samples resulted in zero accumulation of these alkalis. Retaining activity by avoiding alkali poisoning is a significant advantage of the basic catalysts when compared to acidic ones. This stability was demonstrated with the MgO-40 sample, which retained its basicity, surface area and activity after the initial break-in period and therefore, showed promise for the use of these materials in industrial processes. The stability of the MgO-40 sample compared to the other MgO catalysts in this work could potentially be attributed to its relatively high SiO_2 content, which gave it rigidity and enhanced its hydrothermal stability. This can be considered an additional advantage, since SiO_2 is considered an impurity in magnesite samples, which translates to even lower manufacturing cost, making it an ideal catalyst for the process of catalytic biomass pyrolysis.

4. Conclusions

MgO catalytic materials derived from natural magnesite via industrial calcination were evaluated for the process of catalytic fast pyrolysis of biomass in a circulating fluidized bed reactor. The evaluation was carried out in a pilot scale unit using three different MgO catalysts with varying textural and basic properties, in comparison to a commercially available ZSM-5. The MgO materials exhibited relatively high catalytic activity for the conversion of the bio-oil vapors. Deoxygenation was achieved through carbon coupling reactions, such as ketonization and aldol condensation, which resulted in increased CO_2 yields compared to the acidic ZSM-5 catalyst, while CO and H_2O yields decreased. This resulted in increased hydrogen recovery in the produced bio-oils and improved fuel properties. The carbon coupling reactions were evident from the 2DGC-TOFMS quantitative analysis of the produced bio-oils that showed increased ketone content, especially cycloketones with 5- or 6-member rings, which were the most stable products formed via the above-mentioned condensation reactions. The transformation of low MW acids and aldehydes to higher MW products closer to liquid fuel range and the retainment of hydrogen in the bio-oil were the main advantages of the MgO materials. On the other hand, the MgO materials led to significantly increased coke formation and loss of valuable carbon. This was attributed to a combination of their basic reactivity with the non-selective mesoporous structure, which allowed the re-condensation of large oxygenated molecules towards coke.

The evaluation of the MgO catalysts on the pilot scale showed an initial stage of rapid deactivation upon introduction in the unit, similar to the behavior of industrial acidic zeolites. However, after this initial stage, very little further loss of surface area was observed and it was concluded that the MgO catalysts reach an equilibrium state after their initial break-in period, in which they maintained a significant portion of their activity. The deactivation mechanism of MgO was quite different compared to the deactivation mechanism of ZSM-5. No alkali deposition was found to take place on the basic MgO samples, even after numerous consecutive runs. Instead, MgO deactivation was attributed to sintering effects caused by the high temperatures (> 650 °C) in the regenerator, as well as to the high coke formation on the catalyst that could lead to hot spots during regeneration.

Overall, the MgO catalysts proved to be a promising, low-cost alternative to commercial acidic zeolites such as ZSM-5, which are considered the state of the art in biomass pyrolysis. Study of their performance in pilot scale confirmed the conclusions reached in a previous lab scale study and clarified the different mechanisms that prevail in deoxygenation of the bio-oil vapors and in catalyst deactivation. Future endeavors should focus on modifying the textural and/or basic properties of these materials in order to decrease coke production and carbon losses and to make them more thermally stable in order to decrease their deactivation over time due to sintering. Another alternative would be to modify a micro/mesoporous zeolite with MgO phases, in order to tune the acidity-basicity of the final catalyst formulation and drive the product selectivity towards the desired pathways where both type of active sites contribute to increased deoxygenation via CO_2 removal and suppressed coke formation. Additionally, further upgrading of MgO produced bio-oils, especially in comparison to ZSM-5 derived bio-oils, via hydrodeoxygenation will showcase the potential of these bio-oils to produce fuels and hydrocarbons while a study of their stability is needed to ascertain they are suitable for storing without degradation of their properties.

Acknowledgements

The authors wish to acknowledge co-funding of this research by European Union- European Regional Development Fund and Greek Ministry of Education/GGET-EYDE-ETAK through program ESPA 2007-2013 / EPAN II / Action “SYNERGASIA-I” (project 09SYN-42-791).

Appendix A. Supplementary data

Supplementary material related to this article can be found, in the online version, at doi:https://doi.org/10.1016/j.apcatb.2018.07.016.

References

[1] H.B. Goyal, D. Seal, R.C. Saxena, Bio-fuels from thermochemical conversion of renewable resources: a review, Renew. Sustain. Energy Rev. 12 (2008) 504–517, https://doi.org/10.1016/J.RSER.2006.07.014.
[2] G.W. Huber, S. Iborra, A. Corma, Synthesis of transportation fuels from biomass:

chemistry, catalysts, and engineering, Chem. Rev. 106 (2006) 4044–4098, https://doi.org/10.1021/cr068360d.
[3] V. Choudhary, S.I. Sandler, D.G. Vlachos, Conversion of xylose to furfural using Lewis and Brønsted acid catalysts in aqueous media, ACS Catal. 2 (2012) 2022–2028, https://doi.org/10.1021/cs300265d.
[4] A.V. Bridgwater, Review of fast pyrolysis of biomass and product upgrading, Biomass Bioenergy 38 (2012) 68–94, https://doi.org/10.1016/j.biombioe.2011.01.048.
[5] S. Xiu, A. Shahbazi, Bio-oil production and upgrading research: a review, Renew. Sustain. Energy Rev. 16 (2012) 4406–4414, https://doi.org/10.1016/j.rser.2012.04.028.
[6] E.F. Iliopoulou, S.D. Stefanidis, K.G. Kalogiannis, A. Delimitis, A.A. Lappas, K.S. Triantafyllidis, Catalytic upgrading of biomass pyrolysis vapors using transition metal-modified ZSM-5 zeolite, Appl. Catal. B Environ. 127 (2012) 281–290, https://doi.org/10.1016/j.apcatb.2012.08.030.
[7] H. Zhang, Y.-T. Cheng, T.P. Vispute, R. Xiao, G.W. Huber, Catalytic conversion of biomass-derived feedstocks into olefins and aromatics with ZSM-5: the hydrogen to carbon effective ratio, Energy Environ. Sci. 4 (2011) 2297, https://doi.org/10.1039/c1ee01230d.
[8] C.H. Ko, S.H. Park, J.K. Jeon, D.J. Suh, K.E. Jeong, Y.K. Park, Upgrading of biofuel by the catalytic deoxygenation of biomass, Korean J. Chem. Eng. 29 (2012) 1657–1665, https://doi.org/10.1007/s11814-012-0199-5.
[9] J. Fermoso, P. Pizarro, J.M. Coronado, D.P. Serrano, Advanced biofuels production by upgrading of pyrolysis bio-oil, Wiley Interdiscip. Rev. Energy Environ. 6 (2017) 1–18, https://doi.org/10.1002/wene.245.
[10] I.A. Vasalos, A.A. Lappas, E.P. Kopalidou, K.G. Kalogiannis, Biomass catalytic pyrolysis: process design and economic analysis, Wiley Interdiscip. Rev. Energy Environ. 5 (2016), https://doi.org/10.1002/wene.192.
[11] K. Wang, K.H. Kim, R.C. Brown, Catalytic pyrolysis of individual components of lignocellulosic biomass, Green Chem. 16 (2014) 727–735, https://doi.org/10.1039/C3GC41288A.
[12] S.D. Stefanidis, K.G. Kalogiannis, E.F. Iliopoulou, A.A. Lappas, P.A. Pilavachi, In-situ upgrading of biomass pyrolysis vapors: catalyst screening on a fixed bed reactor, Bioresour. Technol. 102 (2011), https://doi.org/10.1016/j.biortech.2011.06.032.
[13] J. Adam, M. Blazsó, E. Mészáros, M. Stöcker, M.H. Nilsen, A. Bouzga, J.E. Hustad, M. Grønli, G. Øye, Pyrolysis of biomass in the presence of Al-MCM-41 type catalysts, Fuel 84 (2005) 1494–1502, https://doi.org/10.1016/J.FUEL.2005.02.006.
[14] J. Adam, E. Antonakou, A. Lappas, M. Stöcker, M.H. Nilsen, A. Bouzga, J.E. Hustad, G. Øye, In situ catalytic upgrading of biomass derived fast pyrolysis vapours in a fixed bed reactor using mesoporous materials, Microporous Mesoporous Mater. 96 (2006) 93–101, https://doi.org/10.1016/J.MICROMESO.2006.06.021.
[15] M.H. Nilsen, E. Antonakou, A. Bouzga, A. Lappas, K. Mathisen, M. Stöcker, Investigation of the effect of metal sites in Me–Al-MCM-41 (Me = Fe, Cu or Zn) on the catalytic behavior during the pyrolysis of wooden based biomass, Microporous Mesoporous Mater. 105 (2007) 189–203, https://doi.org/10.1016/J.MICROMESO.2007.05.059.
[16] J. Jae, G.A. Tompsett, A.J. Foster, K.D. Hammond, S.M. Auerbach, R.F. Lobo, G.W. Huber, Investigation into the shape selectivity of zeolite catalysts for biomass conversion, J. Catal. 279 (2011) 257–268, https://doi.org/10.1016/j.jcat.2011.01.019.
[17] S.D. Stefanidis, K.G. Kalogiannis, P.A. Pilavachi, C.M. Fougret, E. Jordan, A.A. Lappas, Catalyst hydrothermal deactivation and metal contamination during the in situ catalytic pyrolysis of biomass, Catal. Sci. Technol. 6 (2016), https://doi.org/10.1039/c5cy02239h.
[18] M. Nokkosmäki, E. Kuoppala, E. Leppämäki, A.O. Krause, Catalytic conversion of biomass pyrolysis vapours with zinc oxide, J. Anal. Appl. Pyrolysis 55 (2000) 119–131, https://doi.org/10.1016/S0165-2370(99)00071-6.
[19] Q. Lu, Z.-F. Zhang, C.-Q. Dong, X.-F. Zhu, Catalytic upgrading of biomass fast pyrolysis vapors with nano metal oxides: an analytical Py-GC/MS study, Energies 3 (2010) 1805–1820, https://doi.org/10.3390/en3111805.
[20] Q. Lu, Y. Zhang, Z. Tang, W. Li, X. Zhu, Catalytic upgrading of biomass fast pyrolysis vapors with titania and zirconia/titania based catalysts, Fuel 89 (2010) 2096–2103, https://doi.org/10.1016/J.FUEL.2010.02.030.
[21] S. Ernst, M. Hartmann, S. Sauerbeck, T. Bongers, A novel family of solid basic catalysts obtained by nitridation of crystalline microporous aluminosilicates and aluminophosphates, Appl. Catal. A Gen. 200 (2000) 117–123, https://doi.org/10.1016/S0926-860X(00)00646-3.
[22] T.R. Carlson, G.A. Tompsett, W.C. Conner, G.W. Huber, Aromatic production from catalytic fast pyrolysis of biomass-derived feedstocks, Top. Catal. 52 (2009) 241–252, https://doi.org/10.1007/s11244-008-9160-6.
[23] C.A. Gaertner, J.C. Serrano-Ruiz, D.J. Braden, J.A. Dumesic, Catalytic coupling of carboxylic acids by ketonization as a processing step in biomass conversion, J. Catal. 266 (2009) 71–78, https://doi.org/10.1016/j.jcat.2009.05.015.
[24] S.D. Stefanidis, S.A. Karakoulia, K.G. Kalogiannis, E.F. Iliopoulou, A. Delimitis, H. Yiannoulakis, T. Zampetakis, A.A. Lappas, K.S. Triantafyllidis, Natural magnesium oxide (MgO) catalysts: a cost-effective sustainable alternative to acid zeolites for the in situ upgrading of biomass fast pyrolysis oil, Appl. Catal. B Environ. 196 (2016), https://doi.org/10.1016/j.apcatb.2016.05.031.
[25] E.F. Iliopoulou, S. Stefanidis, K. Kalogiannis, A.C. Psarras, A. Delimitis, K.S. Triantafyllidis, A.A. Lappas, Pilot-scale validation of Co-ZSM-5 catalyst performance in the catalytic upgrading of biomass pyrolysis vapours, Green Chem. 16 (2014), https://doi.org/10.1039/c3gc41575a.
[26] V. Paasikallio, K. Kalogiannis, A. Lappas, J. Lehto, J. Lehtonen, Catalytic fast pyrolysis: influencing bio-oil quality with the catalyst-to-biomass ratio, Energy Technol. 5 (2017), https://doi.org/10.1002/ente.201600094.
[27] K.G. Kalogiannis, S.D. Stefanidis, C.M. Michailof, A.A. Lappas, E. Sj?holm, Pyrolysis of lignin with 2DGC quantification of lignin oil: effect of lignin type, process temperature and ZSM-5 in situ upgrading, J. Anal. Appl. Pyrolysis 115 (2015), https://doi.org/10.1016/j.jaap.2015.08.021.
[28] C. Michailof, T. Sfetsas, S. Stefanidis, K. Kalogiannis, G. Theodoridis, A. Lappas, Quantitative and qualitative analysis of hemicellulose, cellulose and lignin bio-oils by comprehensive two-dimensional gas chromatography with time-of-flight mass spectrometry, J. Chromatogr. A 1369 (2014), https://doi.org/10.1016/j.chroma.2014.10.020.
[29] M. Guisnet, P. Magnoux, Organic chemistry of coke formation, Appl. Catal. A Gen. 212 (2001) 83–96, https://doi.org/10.1016/S0926-860X(00)00845-0.
[30] R. Quintana-Solórzano, J.W. Thybaut, G.B. Marin, R. Lødeng, A. Holmen, Single-event microkinetics for coke formation in catalytic cracking, Catal. Today. 107–108 (2005) 619–629, https://doi.org/10.1016/J.CATTOD.2005.07.036.
[31] S. Du, J.A. Valla, G.M. Bollas, Characteristics and origin of char and coke from fast and slow, catalytic and thermal pyrolysis of biomass and relevant model compounds, Green Chem. 15 (2013) 3214, https://doi.org/10.1039/c3gc41581c.
[32] B. Valle, P. Castaño, M. Olazar, J. Bilbao, A.G. Gayubo, Deactivating species in the transformation of crude bio-oil with methanol into hydrocarbons on a HZSM-5 catalyst, J. Catal. 285 (2012) 304–314, https://doi.org/10.1016/J.JCAT.2011.10.004.
[33] D.P. Serrano, J.A. Melero, G. Morales, J. Iglesias, P. Pizarro, Progress in the design of zeolite catalysts for biomass conversion into biofuels and bio-based chemicals, Catal. Rev. 60 (2018) 1–70, https://doi.org/10.1080/01614940.2017.1389109.
[34] H. Hernando, I. Moreno, J. Fermoso, C. Ochoa-Hernández, P. Pizarro, J.M. Coronado, J. Čejka, D.P. Serrano, Biomass catalytic fast pyrolysis over hierarchical ZSM-5 and Beta zeolites modified with Mg and Zn oxides, Biomass Convers. Biorefinery 7 (2017) 289–304, https://doi.org/10.1007/s13399-017-0266-6.
[35] Y.-T. Cheng, J. Jae, J. Shi, W. Fan, G.W. Huber, Production of renewable aromatic compounds by catalytic fast pyrolysis of lignocellulosic biomass with bifunctional Ga/ZSM-5 catalysts, Angew. Chemie 124 (2012) 1416–1419, https://doi.org/10.1002/ange.201107390.
[36] Conversion of the Pyrolytic Vapor of Radiata Pine over, (2016). https://www.tib.eu/de/suchen/id/citeseerx%3Asid~oai%253Ads2%253Aciteseer%252F57ebaacf006c9624760466a3/Conversion-of-the-Pyrolytic-Vapor-of-Radiata-Pine/ (Accessed 8 December 2017).
[37] M. Crocker (Ed.), Thermochemical Conversion of Biomass to Liquid Fuels and Chemicals, Royal Society of Chemistry, Cambridge, 2010, , https://doi.org/10.1039/9781849732260.
[38] A.K. Ma, S. Chand, 1m Mishra, Disproportionation of toluene to produce benzene and p-xylene –A review, J. Sci. Ind. Res. 60 (April) (2001) 319–327 (Accessed 8 December 2017), http://nopr.niscair.res.in/bitstream/123456789/26478/1/JSIR60(4)319-327.pdf.
[39] Y. Liu, X. Zhou, X. Pang, Y. Jin, X. Meng, X. Zheng, X. Gao, F.-S. Xiao, Improved *para* -xylene selectivity in *meta*- xylene isomerization Over ZSM-5 crystals with relatively Long *b* -axis length, ChemCatChem 5 (2013) 1517–1523, https://doi.org/10.1002/cctc.201200691.
[40] C. Tessini, N. Müller, C. Mardones, D. Meier, A. Berg, D. von Baer, Chromatographic approaches for determination of low-molecular mass aldehydes in bio-oil, J. Chromatogr. A 1219 (2012) 154–160, https://doi.org/10.1016/J.CHROMA.2011.10.093.
[41] J.P. Diebold, A Review of the Chemical and Physical Mechanisms of the Storage Stability of Fast Pyrolysis Bio-Oils, (2000) (Accessed 8 December 2017), https://www.nrel.gov/docs/fy00osti/27613.pdf.
[42] Q. Zhang, J. Chang, T. Wang, Y. Xu, Review of biomass pyrolysis oil properties and upgrading research, Energy Convers. Manag. 48 (2007) 87–92, https://doi.org/10.1016/J.ENCONMAN.2006.05.010.
[43] T.N. Pham, T. Sooknoi, S.P. Crossley, D.E. Resasco, Ketonization of carboxylic acids: mechanism, catalysts, and implications for biomass concersion, Am. Chem. Soc. Catal. 3 (2013) 2456–2473.
[44] A. Pulido, B. Oliver-Tomas, M. Renz, M. Boronat, A. Corma, Ketonic decarboxylation reaction mechanism: a combined experimental and DFT study, ChemSusChem 6 (2013) 141–151, https://doi.org/10.1002/cssc.201200419.
[45] L. Rand, W. Wagner, P.O. Warner, L.R. Kovac, Reactions catalyzed by potassium fluoride. II. The conversion of adipic acid to cyclopentanone, J. Org. Chem. 27 (1962) 1034–1035, https://doi.org/10.1021/jo01050a504.
[46] A.T. Nielsen, W.J. Houlihan, A.T. Nielsen, W.J. Houlihan, The aldol condensation, Org. React. John Wiley & Sons, Inc, Hoboken, NJ, USA, 2011, pp. 1–438, https://doi.org/10.1002/0471264180.or016.01.
[47] S.M. Bachrach, Computational Organic Chemistry, (2018) n.d.
[48] C.A. Mullen, A.A. Boateng, Accumulation of inorganic impurities on HZSM-5 zeolites during catalytic fast pyrolysis of switchgrass, Ind. Eng. Chem. Res. 52 (2013) 17156–17161, https://doi.org/10.1021/ie4030209.
[49] V. Paasikallio, C. Lindfors, E. Kuoppala, Y. Solantausta, A. Oasmaa, J. Lehto, J. Lehtonen, Product quality and catalyst deactivation in a four day catalytic fast pyrolysis production run, Green Chem. 16 (2014) 3549, https://doi.org/10.1039/c4gc00571f.